Shen J. Dillon[a], Herb Miller[b], Martin P. Harmer[c], Gregory S. Rohrer[b]
[a] Now at the University of Illinois at Urbana-Champaign, Urbana, IL, U.S.A.
[b] Carnegie Mellon University, Pittsburgh, PA, U.S.A.
[c] Lehigh University, Bethlehem, PA, U.S.A.

Grain boundary plane distributions in aluminas evolving by normal and abnormal grain growth and displaying different complexions

The grain boundary character distributions of selected doped aluminas were measured from normal and abnormal populations. The relative energies of the A-, C-, and R-planes of undoped alumina were also measured. There is an inverse relationship between the population of grain boundaries and the relative energies of grain boundary planes in undoped alumina. This relationship is found to be qualitative for abnormal grains, whose interfacial anisotropy may be affected by kinetic factors. It is found that the relative grain boundary anisotropy correlates with the temperature dependence of grain boundary complexion transitions in a particular system that is prone to abnormal grain growth. However, there is no direct correlation between the total anisotropy of the grain boundary character distribution and that system's propensity to undergo a particular complexion transition. Therefore, anisotropy will significantly affect the microstructural evolution in systems that are prone to abnormal grain growth, but the magnitude of anisotropy is not a sufficient selection criterion for determining which systems will undergo abnormal grain growth.

Keywords: Grain boundary; Grain boundary character; Alumina; Complexion; Abnormal grain growth

1. Introduction

Grain boundaries have associated macroscopic and microscopic degrees of freedom. A grain boundary's character is described by five macroscopically observable parameters; in the most common description, three are related to the misorientation between adjacent grains and two describe the normal to the grain boundary plane. On the microscopic or atomistic scale there are three simple geometric degrees of freedom; two are associated with translation of the grains parallel to the grain boundary plane and one is associated with translations or relaxations normal to the grain boundary plane. The equilibrium configuration of a grain boundary's microscopic degrees of freedom will depend on the macroscopic degrees of freedom, the relevant intensive thermodynamic variables, such as chemical potential, temperature, and pressure. Therefore, grain boundaries of a particular character may undergo structural transitions (first or second order) as a function of chemistry, temperature, etc. It is possible to construct equilibrium grain boundary "phase" diagrams that are analogous to bulk phase diagrams. While the details of the atomic structure will vary significantly with grain boundary character, it has been recognized experimentally that there are certain characteristic equilibrium structures or "phases" that may be stable at grain boundaries. These different characteristic features have been referred to as different complexions [1, 2]. These complexions have thermodynamic stability that relates to the intensive thermodynamic variables, but differ from bulk phases in that they cannot exist in the absence of the abutting crystal. An example of a particular grain boundary complexion is the 1–2 nm intergranular film observed in a number of ceramic materials [3–20]. Complexion transitions may dramatically affect the properties and kinetics of interfaces.

Several different complexions are stable in doped aluminas [1, 21, 22]. The grain boundary mobility varies by orders of magnitude with complexion type and more disordered complexions have higher grain boundary mobilities [1, 23]. The phenomenon of abnormal or discontinuous grain growth in alumina results from different types of complexions coexisting in a single microstructure [1]. Abnormal grain growth describes the growth rate of a grain relative to its neighbors (i.e. it is a differential descriptor). Discontinuous grain growth describes growth of an ensemble of grains whose size distribution does not remain self-similar. The latter descriptor may be more useful, because a microstructure that has undergone a transient stage of abnormal grain growth may arrive at a unimodal grain size distribution, if the number density of abnormal grains is large enough. As a result, "normal grain boundaries" may often result when a significant amount of abnormal grains impinge. In doped aluminas, "normal grain boundaries" may exhibit one of a number of complexions, and the same is true of the "abnormal grain boundaries".

Different complexions may also exist preferentially on specific crystallographic planes in alumina, even on the same grain. This behavior can lead to characteristic grain shapes. Previous studies have indicated that specific dopants influence the relative grain boundary anisotropy in different ways. For example, certain dopants in alumina, such as calcia, anorthite, or lanthana, promote the formation of plate-like grains with large basal planes [24–30]. Other dopants, such as silica or magnesia, promote the formation

of more equiaxed and rounded grains [1, 22, 25, 31–36]. It is difficult to quantify this behavior explicitly through the analysis of grain shape. Anisotropy has often been linked to abnormal grain growth and quantifying the effects should shed new light on the role of anisotropy and chemistry in normal and abnormal grain growth.

The grain boundary character distribution (GBCD) describes the relative areas of interfaces within a microstructure [37]. The GBCD is thought to be a sensitive indicator of materials properties [38–45]. Characterizing the GBCD has been useful for understanding the role of interfacial anisotropy in microstructural evolution of polycrystals during normal grain growth [37, 46–52]. It has also provided insight into anisotropic segregation effects [53–55]. In general, the GBCD has been shown to have an inverse relationship to the distribution of relative grain boundary energies, with low-energy boundaries occurring most frequently and vice versa [37, 47–52]. The GBCD and grain boundary energies are directly correlated for microstructures that have evolved to a steady-state GBCD during normal grain growth [46, 48–52]. The two-parameter GBCD describes the anisotropy in the distribution grain boundary planes in the crystal reference frame [56]. The dynamic range of this distribution provides a good metric for quantifying the relative energy anisotropy of grain boundaries in a system that has evolved by normal grain growth [46].

Recent experiments suggest that the relative anisotropy in the GBCD is important in influencing the frequency with which abnormal grains form (i.e. complexion transitions) as a function of temperature [57]. By controlling the relative anisotropy, it should be possible to engineer the distribution of abnormal grains in a microstructure. For example, this would be important for producing a microstructure of fine grains containing large single crystalline grains that act as reinforcing particles. Alternatively, it might be used to create a uniform microstructure when discontinuous grain growth in unavoidable.

The current work aims to quantify the distribution of grain boundary planes in the crystal reference plane (two-parameter GBCD) and determine how different dopant chemistries affect the relative grain boundary plane anisotropy. The results will be interpreted by comparing the distributions to measured relative energies of specific grain boundary planes. The GBCD will also be used to understand the crystallographic preference of grain boundary complexions.

2. Experimental procedure

A set of samples were produced containing pieces of single crystal sapphire embedded within undoped powder. Single crystals of A-plane, C-plane, and R-plane sapphire were hot-pressed in the undoped powder. The samples were hot-pressed under 50 MPa at 1300 °C for 2 h. The samples were sectioned so that the defined plane was perpendicular to the surface. The sample surface was polished to a 1 micron diamond finish, and was subsequently etched for 2 h at 1350 °C.

The dihedral half angles (Ψ) of thermal grooves were measured for the grain boundaries between the embedded single crystals and the polycrystalline matrix (see schematic in Fig. 1). The dihedral half angles may be used to calculate the relative surface to grain boundary energy in a similar manner to that frequently used for the full dihedral angle [32, 34, 36, 58–69]. In fact, the original analysis by Mullins [70] only considers the groove half angle. Using the half angle on the polycrystal side of the groove avoids introducing artifacts from the surface anisotropy of the single crystal. The grooves were measured using an atomic force microscope in contact mode according to previously established procedures [46, 71].

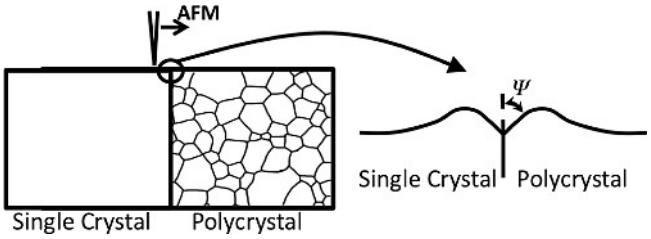

Fig. 1. Schematic of experimental set up for measuring the dihedral half angles at the interface with single crystals of specific geometry.

Dense polycrystals of alumina were prepared by hot-pressing. Undoped alumina (Sumitomo AKP-50, Tokyo, Japan) powder was hot-pressed at 1300 °C for 2 h. Doped alumina powders were prepared by mixing undoped alumina powder with methanol and a dopant precursor. Magnesium nitrate, calcium nitrate, tetraethylorthosilicate, and neodymium nitrate were used as precursors for magnesia, calcia, silica, and neodymia doping, respectively. The powders were mixed, dried and then calcined at ~800 °C for ~24 h. The doped powders were hot-pressed at 1300 °C for 2 h. The samples were sectioned and polished to a 1 μm diamond finish.

The undoped, calcia-doped, magnesia-doped, and silica-doped samples were annealed at 1400 °C for 2 h. The neodymia-doped alumina was annealed at 1400 °C for 50 h in order to coarsen the grains. Under these conditions the samples consisted of almost entirely normal grains, such that abnormal grains were not included in the results. It should be noted that the neodymia- and magnesia-doped alumina were complexion type I for these conditions while the silica- and calcia-doped alumina were predominately complexion type III [1]. The silica- and calcia-doped alumina undergo this transition early in the evolution and at a low temperature, and most of the coarsening has occurred as normal grain growth. A second silica-doped sample was annealed at 1600 °C for 2 h. A second neodymia-doped sample was annealed at 1800 °C for 1 h. A second calcia-doped sample was annealed at 1750 °C for 2 h. These samples were all prepared such that they consisted primarily of impinged abnormal grains, meaning the grain size distribution was somewhat unimodal but was mainly the result of discontinuous grain growth. The samples were repolished to remove thermal grooves that formed during annealing. The samples were then re-annealed at 1200 °C for 2 h in order to remove damage induced during polishing.

Electron back-scatter diffraction (EBSD) (TSL, EDAX Inc.) data was collected in the scanning electron microscope (SEM) (XL 40 FEG, FEI Company). The data were collected at 30 kV with the samples tilted to 70°, at the maximum current attainable without inducing sample charging. The data were collected at a resolution such that at least 10 pixels would span the diameter of the average grain size. The EBSD data were used to confirm that signif-

icant crystallographic texture was not induced during hot-pressing. Reconstructed grain boundary segments were extracted using TSL TexSEM version 5.1. The segments were extracted with a maximum deviation of two pixels between the reconstructed lines and the pixels bounding the interface. These segments define one of the two parameters necessary to define the grain boundary plane. The second parameter is determined for the distribution using a stereological procedure that has been described in detail elsewhere [72, 73].

Approximately 25 000 grains were measured for each sample except for the calcia-doped sample containing only abnormal grains. In this sample, only about 5000 grains were observed due to the large grain size. When the GBCD of the calcia-doped sample was calculated using only portions of the complete set of observations, the result was the same. Therefore, it was assumed 5000 grains are sufficient to determine the distribution. This may be reasonable because of the large amount of anisotropy observed in this distribution.

3. Results

The distribution of dihedral half angles for grains comprised of one A-plane, C-plane, R-plane are plotted in Fig. 2 along with those measured randomly from a distribution of normal grains in the sample. Each of the grain boundaries that is partially comprised of one of the three low index planes measured in alumina (A, C, and R) has a larger median dihedral half angle than those of grains in the random distribution. This indicates that each of these planes has a lower energy than the average of the random population. These data establish a baseline for comparison to the GBCD of undoped alumina. If it is assumed that the median dihedral half angle of the distribution of normal grains is approximately half of the median dihedral angle for that distribution, then the median dihedral angle is 112°. The result is consistent with previous measurements by Handwerker et al. [62], who measured a 112° median dihedral angle for undoped alumina. These results indicate that the basal plane is the lowest energy in undoped alumina. There are conflicting data in the literature as to whether the r-plane or c-plane has the lowest surface energy [74]. The current results are in best agreement with Choi et al. [75].

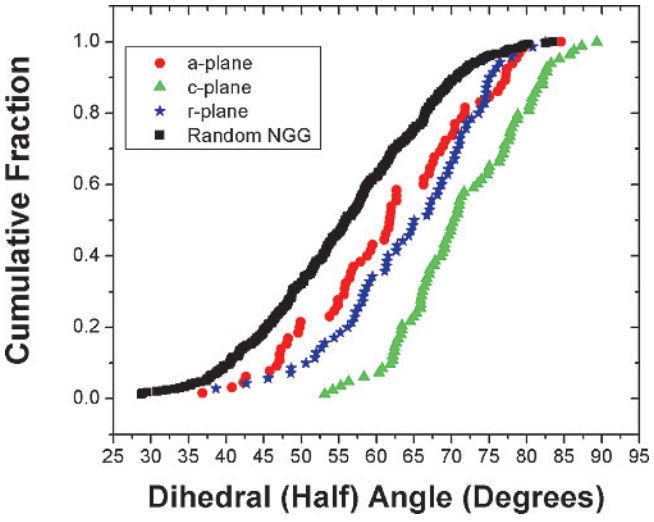

Fig. 2. Distribution of dihedral half angles of random normal grains and a series of grain boundaries made from single crystals of specific crystallographic planes mated with a polycrystal.

Representative maps of EBSD data are shown in Fig. 3. Figure 4 shows the grain boundary plane distributions for the samples annealed at 1400 °C plotted on stereographic projections, all having the same scale. The units of these plots are expressed as multiples of a random distribution. Figure 4 also shows the energies of the c-plane, r-plane, and a-plane, all relative to the energy of the A-plane. These are plotted in a similar manner for easy comparison.

Figure 5 shows the grain boundary plane distributions of neodymia-, silica-, and calcia-doped after abnormal grain growth (i. e. a complexion transition at the majority of grain boundaries). These samples were prepared such that they were composed almost entirely of impinged abnormal grains that had not coarsened significantly after impingement.

4. Discussion

4.1. Anisotropy development during normal grain growth

Comparing the grain boundary plane distribution of the undoped alumina (Fig. 4) to the relative energies of the different planes indicates that there is an inverse relationship between these two quantities. This type of inverse relationship has been noted in several previous studies [37, 47, 56, 76]. Some recent work has established a mechanism by which the GBCD evolves to a steady-state, during normal grain growth, driven by grain boundary energy anisotropy.

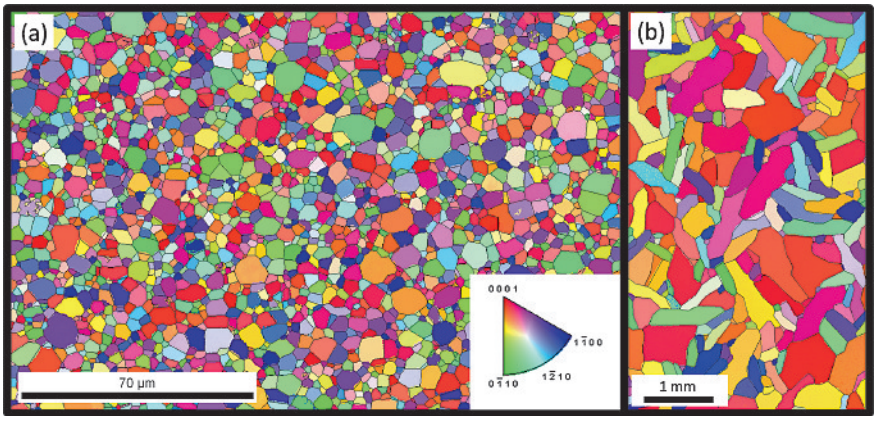

Fig. 3. Orientation Image Map of (a) calcia-doped alumina annealed at 1750 °C for 2 h and (b) undoped alumina annealed at 1400 °C for 2 h.

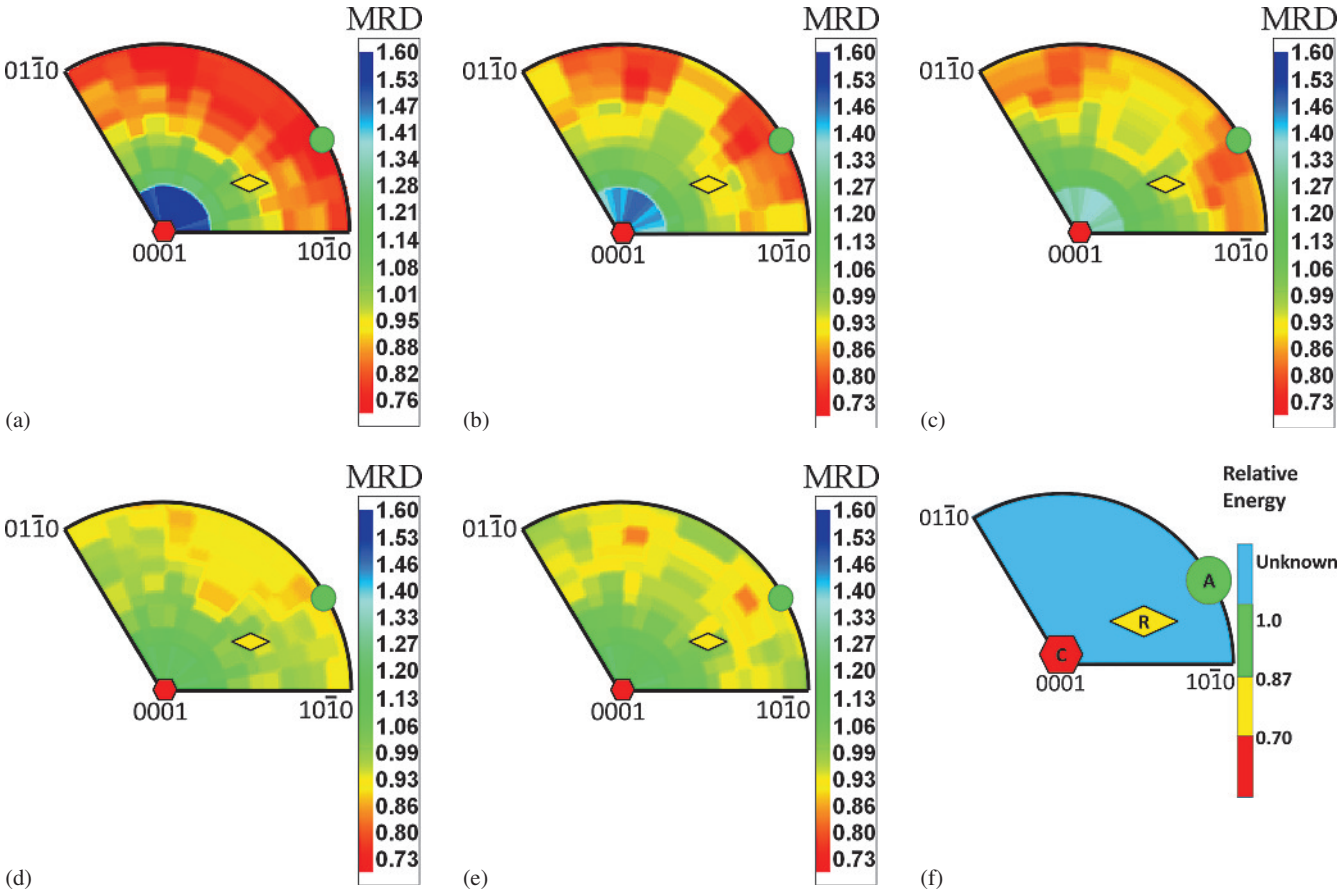

Fig. 4. The distribution of grain boundary plane s for (a) calcia-doped alumina, (b) undoped alumina, (c) silica-doped alumina, (d) magnesia-doped alumina, and (e) neodymia-doped alumina each annealed at 1400 °C and showing normal grain growth. (f) A representation of the relative average energies of several grain boundary planes in undoped alumina.

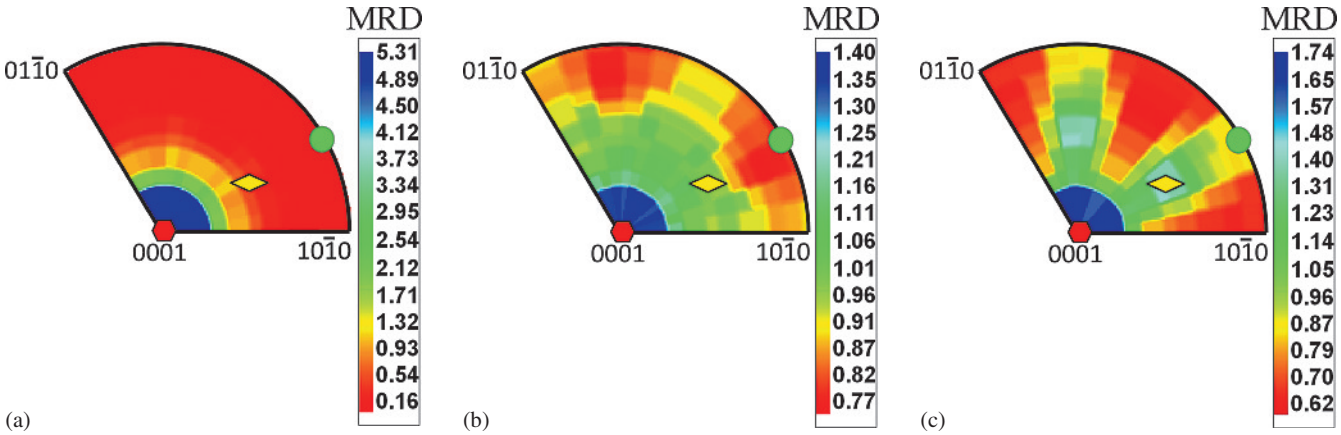

Fig. 5. The distribution of grain boundary planes for (a) calcia-doped alumina annealed at 1750 °C, (b) silica-doped alumina annealed at 1600 °C, and (c) neodymia-doped alumina annealed at 1800 °C.

For this case, there is a direct correlation between the anisotropy in the GBCD and the anisotropy in the grain boundary energy distribution [46, 48, 49].

It should be noted that the relative energies of different planes have only been measured in undoped alumina, in this study. Doping will certainly affect the grain boundary energy distribution. However, the GBCD should be correlated with the grain boundary energy distribution in the microstructures that evolved by normal grain growth. The calcia-doped alumina has the most anisotropic GBCD, followed by the undoped, silica-doped, magnesia-doped, and then neodymia-doped alumina. It has been well known that calcia doping increases the anisotropy of alumina, while magnesia doping reduces it. It has been suggested previously that anisotropy effects alone might lead to abnormal grain growth [34, 77]. The current results suggest that anisotropy effects alone do not predict the occurrence of abnormal grain growth in alumina. For example, neodymia-

doped alumina is relatively isotropic, comparable to magnesia-doped alumina. Neodymia doped alumina shows a strong preference for abnormal grain growth, while magnesia doping suppresses it. Also, silica-doped alumina is more isotropic than undoped alumina and is also highly prone to discontinuous and abnormal grain growth, while the high-purity undoped material is not.

Previous work showed that the number density of abnormal grains in doped alumina increased exponentially with temperature [57]. The slope of this exponential varied with different dopants. It was shown that the temperature range of the transition from normal to abnormal grain growth was much narrower for the case of silica-doped alumina as compared to calcia-doped alumina [57]. It was surmised that the population of boundaries in silica-doped alumina was more isotropic which would cause the individual boundaries to behave similarly, while calcia-doped alumina was more anisotropic which would cause the behavior of its boundaries to be more diverse (i.e. spread over a larger temperature range). The current results support that hypothesis, which suggests anisotropy in the normal population will play an important role in determining the evolution of the abnormal population.

4.2. Anisotropy development during abnormal grain growth

Figure 5 shows the grain boundary plane distributions of neodymia-, silica-, and calcia-doped alumina after abnormal grain growth (i.e. a complexion transition at the majority of grain boundaries). When compared to the distributions before the complexion transition, each material behaves differently. The anisotropy in the GBCD for silica-doped alumina before and after abnormal grain growth is the same within expected uncertainty. This is consistent with the fact that the abnormal grains in silica-doped alumina are relatively equiaxed and the boundaries are curved. The anisotropy of the GBCD for neodymia-doped alumina is increased as a result of abnormal grain growth, with new peaks in the distribution occurring at the orientation of the rhombohedral planes. In the neodymia-doped alumina, both the basal planes and the rhombohedra planes are faceted and grow relatively quickly during abnormal grain growth [78]. The anisotropy of the GBCD for calcia-doped alumina increases dramatically during abnormal grain growth. A significant change in the GBCD could result from either a change in the grain boundary energy distribution associated with the complexion transition or from kinetic factors that favor certain grain boundary planes. In the latter case, the GBCD may deviate significantly from what would be predicted as the steady-state distribution.

Previous measurements of dihedral angles at thermal grooves in calcia-doped alumina indicated that the basal plane energy on abnormal grains at 1400 °C is ~25 % lower than the average of the other planes on the same abnormal grains [79]. This is comparable to the amount of anisotropy observed in the undoped alumina. Therefore, the energy anisotropy alone cannot explain the large anisotropy in the GBCD. The large anisotropy in the abnormal distribution of the calcia-doped alumina likely results from the fact that complexion transitions occur preferentially on different planes in this alumina, and this results in a large mobility anisotropy. Specifically, Complexion transitions are less likely to occur on basal planes than the plane perpendicular. The basal planes advance relatively slowly, whiles the planes perpendicular to the basal plane advance rapidly and this creates plate-shaped grains. These results indicate that the grain boundary plane distribution will be influenced by kinetic preferences during abnormal grain growth.

The results of numerous simulations of untextured polycrystals show that only grain boundary energy anisotropy is effective in producing large anisotropy in the GBCD, while mobility anisotropy has little effect [48, 50–52, 80]. The simulations have the common feature that boundaries of a particular misorientation or character are assigned a single energy and mobility. Because of this, these simulations do not provide an accurate description of the mobility anisotropies that result from complexion transitions. In the simulation, a boundary that is advancing rapidly will change its character as soon as it moves through a neighboring grain. When this happens, the boundary immediately loses its mobility advantage (except in the unlikely event that its new character also has a high mobility). Boundaries that have undergone a complexion transition, on the other hand, have high mobilities because of their composition and structure rather than their crystallographic character. While it is not possible to sustain a single grain boundary character during growth, it is possible to sustain the composition and structure of a complexion as the grain boundary advances. So, while grain boundary mobility anisotropy does not influence the GBCD during normal grain growth, it can be influential during abnormal grain growth.

Experimental results indicate that a particular complexion will exist on multiple grain boundaries bounding an individual grain. As a result, the large differences in mobility are correlated with individual grains rather than individual grain boundaries. Because the grain growth simulations that incorporate mobility anisotropy are based on mechanisms that cannot reproduce this experimental observation, their inability to produce GBCDs that are affected by mobility anisotropy is not surprising. The character of boundaries surrounding an abnormal grain will vary continuously as it grows, but if the grain has a preferred shape then an anisotropic GBCD will result. In this case, there are two interesting possibilities. If the all of the boundaries around a grain have high mobility and there are preferred habit planes, then the orientation of the boundaries with the high mobility complexion will dominate the GBCD. On the other hand, if only some of the boundaries have high mobilities, then they advance rapidly, extending the area of the low mobility boundaries, and the GBCD is dominated by the low mobility planes. This is what occurs in calcia-doped alumina when the high mobility prismatic facets advance rapidly, extending the area of the low mobility basal facet that eventually dominates the GBCD. Therefore, mobility effects can be expressed in the GBCD, but there are several possibilities and this may be the reason why the GBCDs of silica-, neodymia-, and calcia-doped alumina change in different ways as a result of the complexion transition.

For a particular complexion to be correlated to an abnormally growing grain, the complexions on some of either the normal or abnormal grain boundaries must be metastable (i.e. two boundaries with the same crystallographic character can have two distinct mobilities or complexions). The idea of complexion metastability has been noted and discussed previously [81]. The metastability is believed to result from the difference in composition between two differ-

ent saturated complexions that might exist on the same type of boundary, and a steady-state chemistry established during migration. When the anisotropy in the GBCD is influenced by kinetic effects, then it is not quantitatively linked to the grain boundary energy distribution. However, the GBCD results presented here suggests that a qualitative correlation remains.

The results also indicate that the grain boundary plane anisotropy prior to abnormal grain growth is not a reliable indicator of anisotropy after abnormal grain growth. The differences in growth preference resulting from complexion transitions in different chemistries are likely linked to preferred atomic-scale energetics, structures, and configurations. Anisotropy in precipitation and segregation should also be important factors. The relative anisotropy appears to be important in affecting the temperature dependence of certain complexion transitions, and is critically important in the final morphology and microstructure. Because of this, a deeper understanding of these anisotropy effects and how they link with the atomic scale is important in developing thorough models of microstructural evolution.

5. Conclusions

Additives significantly influence the anisotropy in the GBCD of alumina. The results support a prior claim that grain boundary anisotropy should affect the temperature dependence of grain boundary complexion transitions that induce abnormal grain growth. However, the magnitude of the anisotropy is not a sufficient metric to determine whether or not a particular system will undergo discontinuous or abnormal grain growth.

It has been shown that for microstructures that evolve by abnormal or discontinuous grain growth, there is a qualitative inverse relationship between grain boundary energy anisotropy and the GBCD. However, energy effects alone cannot quantitatively justify the magnitude of the grain boundary character anisotropy in certain cases. For abnormal grain growth, the relative grain boundary mobilities appear to play an important role. This differs from normal grain growth, where it has been previously shown that the anisotropy in the GBCD may be predicted directly from the grain boundary energy anisotropy with almost no influence of mobility anisotropy. The growth preference of abnormal grains does not appear to be easily predicted from the anisotropy of the normal grains prior to abnormal growth. A better understanding of the links between grain boundary character and atomistic aspects of grain boundary complexions is likely required to understand these effects.

This work was supported the Pennsylvania DCED and by the MRSEC program of the National Science Foundation under Award Number DMR-0520425.

References

[1] S.J. Dillon, M. Tang, W.C. Carter, M.P. Harmer: Acta Mater. 55 (2007) 6208. DOI:
[2] M. Tang, W.C. Carter, R.M. Cannon: Phys. Rev. B: Condens. Matter and Materials Physics. 73 (2006) 024102/1. DOI:
[3] D.R. Clarke: Ultramicroscopy 4 (1979) 33. DOI:
[4] D.W. Susnitzky, C.B. Carter: J. Am. Ceram. Soc. 73 (1990) 2485. DOI:
[5] M.K. Cinibulk, H.J. Kleebe, G.A. Schneider, M. Rühle: J. Am. Ceram. Soc. 76 (1993) 2801. DOI:
[6] H.J. Kleebe, M.K. Cinibulk, R.M. Cannon, M. Rühle: J. Am. Ceram. Soc. 76 (1993) 1969. DOI:
[7] I. Tanaka, H.-J. Kleebe, M.K. Cinibulk, J. Bruley, D.R. Clarke, M. Rühle: J. Am. Ceram. Soc. 77 (1994) 911.
[8] H. Gu, X. Pan, I. Tanaka, R.M. Cannon, M.J. Hoffmann, H. Muellejans, M. Rühle. Mat. Sci. Forum 207–209 (1996) 729. DOI:
[9] Y.M. Chiang, H. Wang, J.R. Lee: Journal of Microscopy (Oxford). 191 (1998) 275. DOI:
[10] R.O. Ritchie, X.F. Zhang, L.C. de Jonghe: Materials Research Society Symposium Proceedings 819 (2004) 3. DOI:
[11] A. Avishai, C. Scheu, W.D. Kaplan: Acta Mater. 53 (2005) 1559. DOI:
[12] M. Baram, W.D. Kaplan: J. Mater. Sci. 41 (2006) 7775. DOI:
[13] R. Wirth: Contrib. Mineral. Petrol. 124 (1996) 44. DOI:
[14] H.D. Ackler, Y.-M. Chiang: J. Am. Ceram. Soc. 80 (1997) 1893. DOI:
[15] L. Franz, R. Wirth: Contrib. Mineral. Petrol. 129 (1997) 268. DOI:
[16] R.R. Brydson, S.-C. Chen, F.L. Riley, S.M.-X. Pan, M. Rühle: J. Am. Ceram. Soc. 81 (1998) 369. DOI:
[17] O.S. Kwon, S.H. Hong, J.H. Lee, U.J. Chung, D.Y. Kim, N.M. Hwang: Acta Mater. 50 (2002) 4865. DOI:
[18] S.-Y. Chung, S.-J.L. Kang: Acta Mater. 51 (2003) 2345. DOI:
[19] H. Qian, J. Luo: Appl. Phys. Lett. 91 (2007) 061909. DOI:
[20] H. Qian, J. Luo, Y.-M. Chiang: Acta Mater. 56 (2008) 862. DOI:
[21] S.J. Dillon, M.P. Harmer: J. Am. Ceram. Soc. 91 (2008) 2304. DOI:
[22] S.J. Dillon, M.P. Harmer: J. Am. Ceram. Soc. 91 (2008) 2314. DOI:
[23] S.J. Dillon, M.P. Harmer: Acta Mater. 55 (2007) 5247. DOI:
[24] S. Baik, C.L. White: J. Am. Ceram. Soc. 70 (1987) 682. DOI:
[25] S. Baik, J.H. Moon: J. Am. Ceram. Soc. 74 (1991) 819. DOI:
[26] W.D. Kaplan, H. Muellejans, M. Rühle, J. Roedel, N. Claussen: J. Am. Ceram. Soc. 78 (1995) 2841. DOI:
[27] J. Cho, C.M. Wang, H.M. Chan, J.M. Rickman, M.P. Harmer: J. Mater. Res. 16 (2001) 425. DOI:
[28] J. Cho, C.M. Wang, H.M. Chan, J.M. Rickman, M.P. Harmer: Acta Mater. 47 (1999) 4197. DOI:
[29] J.-K. Park, D.-Y. Kim, H.-Y. Lee, J. Blendell, C. Handwerker: J. Am. Ceram. Soc. 86 (2003) 1014. DOI:
[30] S.-H. Lee, D.-Y. Kim, N.M. Hwang: J. Eur. Ceram. Soc. 22 (2002) 317. DOI:
[31] K.L. Gavrilov, S.J. Bennison, K.R. Mikeska, J.M. Chabala, R. Levi-Setti: J. Am. Ceram. Soc. 82 (1999) 1001. DOI:
[32] S. Baik: J. Am. Ceram. Soc. 69 (1986) C101. DOI:
[33] C.W. Park, D.Y. Yoon: J. Am. Ceram. Soc. 84 (2001) 456. DOI:
[34] S.J. Bennison, M.P. Harmer: Ceramic Transactions. 7 (1990) 13. DOI:
[35] G.S. Thompson, P.A. Henderson, M.P. Harmer, G.C. Wei, W.H. Rhodes: J. Am. Ceram. Soc. 87 (2004) 1879. DOI:
[36] I. MacLaren, R.M. Cannon, M.A. Gülgün, R. Voytovych, N. Popescu-Pogrion, C. Scheu, U. Täffner, M. Rühle: J. Am. Ceram. Soc. 86 (2003) 650. DOI:

[37] D.M. Saylor, A. Morawiec, G.S. Rohrer: Acta Mater. 51 (2003) 3663. DOI:
[38] S. Kobayashi, T. Inomata, H. Kobayashi, S. Tsurekawa, T. Watanabe: J. Mater. Sci. 43 (2008) 3792. DOI:
[39] L. Tan, K. Sridharan, T.R. Allen, R.K. Nanstad, D.A. McClintock: J. Nucl. Mater. 374 (2008) 270. DOI:
[40] Y. Chen, C.A. Schuh: Phys. Rev. B. Condens. Matter and Materials Physics. 76 (2007) 064111/1. DOI:
[41] H. Kokawa, M. Shimada, M. Michiuchi, Z.J. Wang, Y.S. Sato: Acta Mater. 55 (2007) 5401. DOI:
[42] L. Tan, K. Sridharan, T.R. Allen: J. Nucl. Mater. 371 (2007) 171. DOI:
[43] T. Watanabe, S. Tsurekawa: Mater. Sci. Eng. A: Structural Materials: Properties, Microstructure and Processing. A387–A389 (2004) 447. DOI:
[44] S. Tsurekawa, T. Watanabe, H. Watanabe, N. Tamari*:* Key Eng. Mater. 247 (2003) 327. DOI:
[45] M. Shimada, H. Kokawa, Z.J. Wang, Y.S. Sato, I. Karibe: Acta Mater. 50 (2002) 2331. DOI:
[46] S.J. Dillon, G.S. Rohrer: Acta Mater. in Press (2008). DOI:
[47] D.M. Saylor, A. Morawiec, G.S. Rohrer: Acta Mater. 51 (2003) 3675. DOI:
[48] J. Gruber, D.C. George, A.P. Kuprat, G.S. Rohrer, A.D. Rollett: Scripta Mater. 53 (2005) 351. DOI:
[49] G.S. Rohrer, J. Gruber, A.D. Rollett: Proceedings of the 15th International Conference on Texture of Materials. submitted (2007). DOI:
[50] E.A. Holm, G.N. Hassold, M.A. Miodownik: Acta Mater. 49 (2001) 2981. DOI:
[51] G.N. Hassold, E.A. Holm, M.A. Miodownik: Mater. Sci. Technol. 19 (2003) 683. DOI:
[52] U. Upmanyu, G.N. Hassold, A. Kazaryan, E.A. Holm, Y. Wang, B. Patton, D.J. Srolovitz: Interface Sci. 10 (2002) 201. DOI:
[53] Y. Pang, P. Wynblatt: J. Am. Ceram. Soc. 89 (2006) 666. DOI:
[54] F. Papillon, P. Wynblatt, G.S. Rohrer: Mater. Sci. Forum 467–470 (2004) 789. DOI:
[55] P. Wynblatt, Z. Shi: J. Mater. Sci. 40 (2005) 2765. DOI:
[56] D.M. Saylor, B. El Dasher, Y. Pang, H.M. Miller, P. Wynblatt, A.D. Rollett, G.S. Rohrer: J. Am. Ceram. Soc. 87 (2004) 724. DOI:
[57] S.J. Dillon, M.P. Harmer: J. Eur. Ceram. Soc. (2008). DOI:
[58] R.D. Monahan, J.W. Halloran: J. Am. Ceram. Soc. 62 (1979) 564. DOI:
[59] K.J. Morrissey, C.B. Carter: J. Am. Ceram. Soc. 67 (1984) 292. DOI:
[60] K.A. Berry, M.P. Harmer: J. Am. Ceram. Soc. 69 (1986) 143. DOI:
[61] R.F. Cook, A.G. Schrott: J. Am. Ceram. Soc. 71 (1988) 50. DOI:
[62] C.A. Handwerker, J.M. Dynys, R.M. Cannon, R.L. Coble: J. Am. Ceram. Soc. 73 (1990) 1371. DOI:
[63] J. Rödel, A.M. Glaeser: J. Am. Ceram. Soc. 73 (1990) 3292. DOI:
[64] H. Song, R. Coble: J. Am. Ceram. Soc. 73 (1990) 2086. DOI:
[65] A. Kebbede, G.L. Messing, A.H. Carim: J. Am. Ceram. Soc. 80 (1997) 2814. DOI:
[66] J. Tartaj, G.L. Messing: J. Eur. Ceram. Soc. 17 (1997) 719. DOI:
[67] Y.-M. Kim, S.-H. Hong, D.-Y. Kim: J. Am. Ceram. Soc. 83 (2000) 2809. DOI:
[68] G.S. Cargill, III, C.M. Wang, J.M. Rickman, H.M. Chan, M.P. Harmer: Materials Research Society Symposium Proceedings. 654 (2001) AA1 1/1. DOI:
[69] C.-M. Wang, J. Cho, H.M. Chan, M.P. Harmer, J.M. Rickman: J. Am. Ceram. Soc. 84 (2001) 1010. DOI:
[70] W.W. Mullins: J. Appl. Phys. 28 (1957) 333. DOI:
[71] D.M. Saylor, G.S. Rohrer: J. Am. Ceram. Soc. 82 (1999) 1529. DOI:
[72] D.M. Saylor, B.S. El-Dasher, B.L. Adams, G.S. Rohrer: Metall. Mater. Trans. A 35 (2004) 1981. DOI:
[73] D.M. Saylor, G.S. Rohrer: J. Am. Ceram. Soc. 85 (2002) 2799. DOI:
[74] M. Kitayama, A.M. Glaeser: J. Am. Ceram. Soc. 85 (2002) 611. DOI:
[75] J.-H. Choi, D.-Y. Kim, B.J. Hockey, S.M. Wiederhorn, C.A. Handwerker, J.E. Blendell, W.C. Carter, A.R. Roosen: J. Am. Ceram. Soc. 80 (1997) 62. DOI:
[76] D.M. Saylor, B. El Dasher, T. Sano, G.S. Rohrer: J. Am. Ceram. Soc. 87 (2004) 670. DOI:
[77] W. Yang, L.-Q. Chen, G.L. Messing: Mat. Sci. Eng. A 195 (1995) 179. DOI:
[78] S.J. Dillon, M.P. Harmer: J. Am. Ceram. Soc. 90 (2007) 996. DOI:
[79] S.J. Dillon, M.P. Harmer, G.S. Rohrer: J. Am. Ceram. Soc., in preparation (2008). DOI:
[80] D. Kinderlehrer, I. Livshits, G.S. Rohrer, S. Ta'asan, P. Yu: Mater. Sci. Forum 467–470 (2004) 1063. DOI:
[81] S.J. Dillon, M.P. Harmer: J. Eur. Ceram. Soc. 28 (2008) 1485. DOI:

(Received April 7, 2009; accepted November 3, 2009)

Bibliography

DOI 10.3139/146.110253
Int. J. Mat. Res. (formerly Z. Metallkd.)
101 (2010) 1; page 1–7

ISSN 1862-5282

Correspondence address

Prof. Gregory S. Rohrer
Department of Materials Science and Engineering
Carnegie Mellon University
5000 Forbes Avenue
Pittsburgh, PA 15213–3890, U.S.A.
Tel.: +412 268 2696
Fax: +412 268 3113
E-mail: gr20@andrew.cmu.edu